https://doi.org/10.1142/9789811278952_0016

Chapter 16

11T Dipole and New Connection Cryostats for Collimators

Bernardo Bordini, Luca Bottura, Arnaud Devred, Lucio Fiscarelli,
Mikko Karppinen, Gijs de Rijk, Lucio Rossi, Frédéric Savary,
Daniel Schörling and Gerard Willering

CERN, Geneva 23, CH-1211, Switzerland

This chapter describes the design of, and parameters for, the 11 T dipole [11] developed at FNAL and the European Organization for Nuclear Research (CERN) for the High Luminosity Large Hadron Collider (HL-LHC) project.

1. Introduction

The HL-LHC upgrade will yield a more intense proton beam, with a circulating current of 1.1 A per beam vs. the 0.56 A nominal current value in the LHC. The intensity of the ion beams (usually Pb ions) for ion–ion collisions will actually be increased by a factor of three: from $4*10^{10}$ to $1.2*10^{11}$ circulating particles per beam. This intensity increase, both for protons and ions, will increase the diffractive losses at the primary collimators, located in LHC Point 7 (P7), which may drive the energy deposition in the main dipoles located in the dispersion suppressor (DS) region above the quench limit. To avoid limiting the machine due to this effect, various countermeasures have been studied, and the solution chosen was to intercept these diffractive losses via warm absorbers (also called collimators) placed in the cold dispersion suppressor region of the LHC. The most elegant and practical way to introduce a room-temperature zone in the DS, at a location corresponding to the middle of the second dipole of the DS cell, was to substitute a regular LHC dipole (8.33 T of central field and 14.3 m of magnetic length) with a magnet of 11 T

with a length of approximately 11 m, yielding the same bending strength while saving about 3.5 m of longitudinal space. The 11 T field in the magnet bore inevitably calls for Nb_3Sn technology. The space gained, thanks to the higher field and shorter length, is sufficient to insert a cold–warm–cold bypass on which to allocate all lines for cryogenic and electrical continuity of the circuits being powered in series throughout the LHC arc, as well as to install the Target Collimator Long Dispersion suppressor (TCLD). For reasons of beam dynamics and to reduce the technology risk associated with the innovative and relatively expensive Nb_3Sn superconductor, the 11 T dipole was split into two magnets of 5.5 m length, with the bypass and collimator installed in the middle. A schematic layout of the assembly with its position in the LHC is shown in Figure 1.

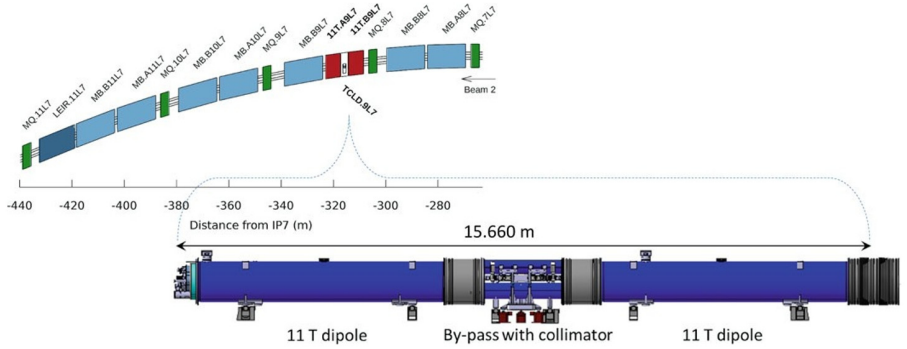

Fig. 1. Schematic of the 11 T cryo-assembly, with the bypass hosting the collimator at the center. In the dispersion suppressor (DS) cells (the array in the topwhere LHC dipoles are in light blue) one standard dipole is replaced by the 11 T cryo-assembly, indicated in red.

A similar DS cleaning upgrade is required for heavy ion collisions in the ALICE experiment of IP2, where secondary ion beams with different magnetic rigidity are created, which are lost in the adjacent DS. These secondary ion beams create heat deposition in the impacted magnet that could lead to a magnet quench. Bound-free pair production (BFPP) are the dominant process with the main heat deposition occurring in Cell 10 of the long arc cryostat. The same TCLD collimator assembly as foreseen for IR7 has therefore been installed as cold-warm-cold transition just without the 11 T dipole magnets on either side of IR2, replacing the previous connection cryostat in Cell 10 (see Figure 2).

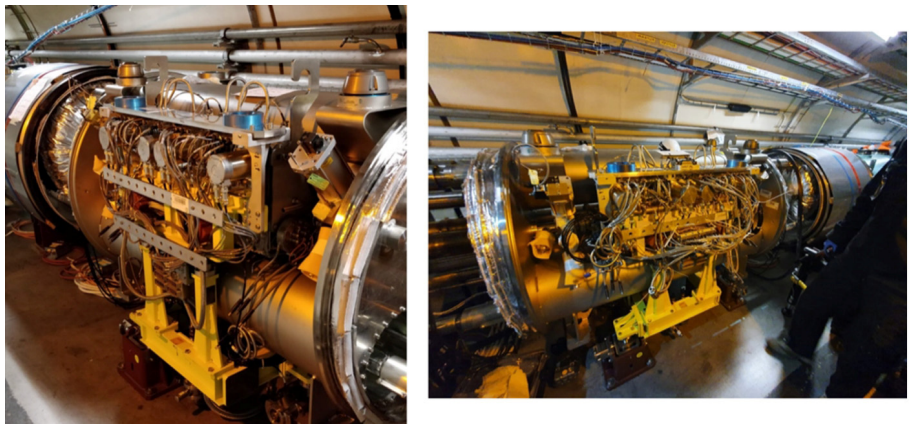

Fig. 2. TCLD assembly installed along with new connection cryostats on either side in Cell 10 of IR2, replacing the former empty connection cryostat.

2. Magnet Design

The main constraint of the 11 T magnet design stems from the fact that the 11 T dipole pair becomes a part of the LHC main circuits of the LHC sectors 67 and 78 and, as such, is powered in series with the remaining 153 LHC two-in-one- aperture dipole magnets. Each 11 T dipole magnet pair therefore must provide an integrated transfer function (ITF) as close as possible to that of the LHC main dipole magnets over the whole dynamic range, from injection energy of 0.45 TeV (7.7 T.m of bending strength) to the collision energy of 7 TeV (119.2 T.m of bending strength). These values for the bending strength must be obtained at the nominal current of the main bending (MB) circuit, *i.e.*, 760 A at the 0.45 TeV injection energy and 11.85 kA at the 7 TeV collision energy. A second condition was to respect the LHC's basic geometry: the distance between the center of the two apertures (194 mm at 1.9 K) and the position of the cryogenic and electrical lines passing through the yoke. Finally, the timescale did not allow for a long period of R&D. It was therefore decided to rely on a design concept as close as possible to that of the LHC MB dipoles, from which CERN has accumulated more than two decades of experience [1]: the two-layer cos-theta coil layout, with the force supported by a classical collar structure, a vertically split iron yoke, and an external shrinking cylinder also serving as a helium vessel. Thanks to CERN's experience and to the

FNAL program on the Nb_3Sn cos-theta layout with collars, the initial decision on the layout was taken [2,3,13].

The preliminary design study proved that all main design criteria, *i.e.*, field strength with a reasonable ITF over all of the dynamic range, critical current margin, and field quality (both at injection and at high field), could be met with the available Nb_3Sn wire properties, despite the considerable difficulties given by the various constraints. Structural and protection issues were left to a later, more detailed and realistic design.

2.1. *Basic design Features*

Different from the LHC main dipole magnets, the 11 T dipole magnets feature separate stainless-steel collars for each aperture, compared to common stainless-steel collars in the case of the LHC MBs. This design change was introduced to allow a better-controlled symmetric loading of the coils and make it possible to test the collared coils in a one-in-one configuration without the need for de-collaring prior to integration in the two-in-one cold mass. To maximize the use of the existing infrastructure and cold-mass assembly tooling, the outer contour of the cold mass was chosen to be identical to the LHC MBs. The location and the section of the slots' busbars was to be preserved, as well as the location of the heat exchanger in the iron yoke.

A nominal field of 11 T requires a magnet that is about 11 m long. To reduce the risks associated with the fabrication of brittle Nb_3Sn coils, the original 11 m long magnet was split into two units, each 5.5 m long and with straight coils, not being bent as the ones of the LHC MBs. The sagitta of the beam trajectory in each of the two 5.5 m long straight magnets is only around 2 mm, compared to 9 mm in a standard LHC MB. During the initial phase of the project, it was considered important to compensate for the effect of the sagitta on the free aperture by enlarging the coil aperture to 60 mm (compared to the 56 mm in the LHC MB). Later, it was however decided to use existing spare beam screens from the LHC without an increased free aperture.

The field quality targets were similar to those of the LHC MB, *i.e.*, at the 10^{-4} level at the reference radius of 17 mm. Special attention had however to be paid to the multipoles arising from persistent currents induced in the inherently larger filaments of the available Nb_3Sn strands and the higher

yoke saturation (with a larger magnetic flux conveyed in the same yoke as the LHC MB).

A further important advantage of this solution is the possibility of placing the collimator between the two 5.5 m long 11 T dipoles, reducing the orbit excursion.

To ensure reliable operation, the design goal was to provide an operational margin of 20% on the load line, as for other Nb_3Sn HL-LHC magnets, assuming that the only conductor performance degradation results from cabling and neglecting transverse stress effects. The initial design of the 11 T dipole is described in [2] and [3].

2.2. *Conductor Choice and nominal dimensions*

The parameters of the strands and the Rutherford cable were selected based on the required number of ampere-turns to generate the requested ITF under the 20% operating margin, the available coil space, and the maximum number of strands possible in the cabling machine. The finally selected strand diameter was 0.7 mm, with an expected cable thickness in the range of 1.2–1.3 mm (depending on the allowed compaction). The strand geometry and performance specification are summarized in Table 1.

The optimization of cable parameters was done jointly by FNAL and CERN [3] and included the selection of the cable cross-section geometry and compaction to achieve good mechanical stability of the cable and acceptable I_C degradation (less than 10%), incorporating a stainless-steel core (25 μm thickness), and preserving a high residual resistivity ratio (RRR) of the Cu matrix (RRR larger than 100 in extracted strands) as given in Table 2 and depicted in Figure 3.

Table 1. Nb_3Sn wire geometry and specifications

Description	Value
Strand diameter (mm)	0.70
J_c (12 T, 4.2 K) (kA/mm^2)	> 2.45
Effective filament size D_{eff} (μm)	< 41
Twist pitch (mm)	14
Cu RRR (virgin state)	> 150
Cu-to-non-Cu fraction (%)	53.5 (±2)

Table 2. Cable geometrical parameters

Parameter	Reacted	Unreacted
Mid-thickness (mm)	1.25	1.30
Thin edge (mm)	1.15	1.19
Thick edge (mm)	1.35	1.40
Width (mm)	14.70	15.08
Keystone angle (o)	0.79	0.81

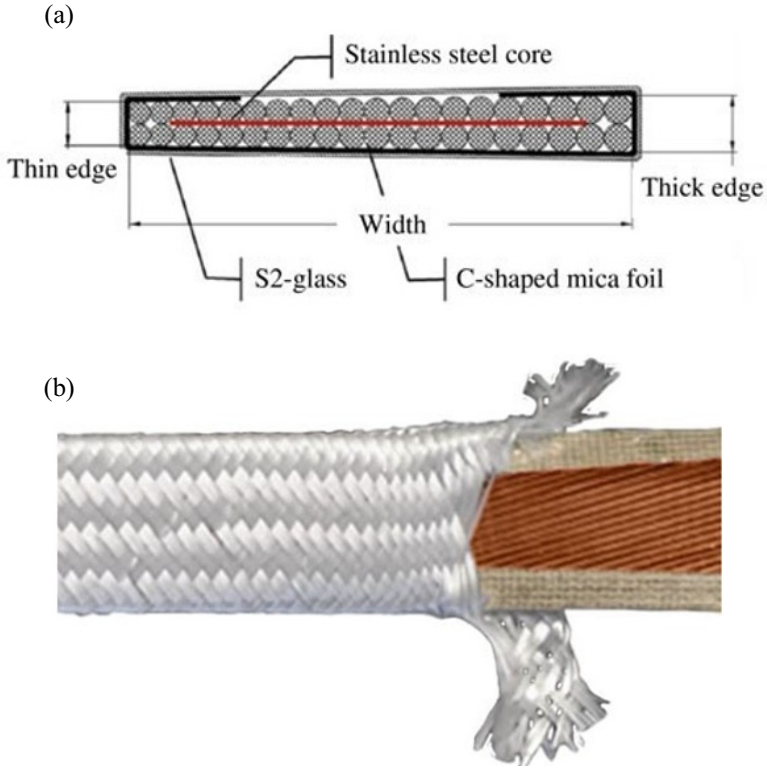

Fig. 3. Cable insulation based on S2-glass braided on mica tape (CERN insulation): (a) schematic; and (b) photograph.

The choice of filament results on the contrary in a significantly higher magnetic induction heating, being at compatible with the available cryogenic power only for a small number of magnets to be installed in the LHC [12].

2.3. *Magnetic Design*

The main electromagnetic design challenges of the two-in-one-aperture 11 T dipole magnet are to match the integrated transfer function of the MB, to control the magnetic crosstalk between apertures, and to minimize the magnitude and variation of non-allowed multipoles [4]. The coil cross-section was optimized using the reacted cable parameters and a 100 μm insulation layer around the cable. The early-stage preliminary design used the iron yoke shown in Figure 4(a), leaving a radial space of about 30 mm for the collars. The optimal configuration, delivering 11.21 T at 11.85 kA in a two-in-one configuration, was found with a six-block layout of 56 turns with 22 turns in the inner layer and 34 turns in the outer layer, as shown in Figure 4(b).

The coil ends were optimized first to find the optimal mechanical configuration based on easy- and hard-way strain in the cable, as well as the amount of torsion over the unit length. The lead-end optimization also included the layer jump and the transitions between the winding blocks. The relative axial positions of the end blocks were then optimized to minimize the integrated harmonics.

It was decided to use this coil design for the short models and then, before scaling up to the full length, re-optimize the coil cross-section with the experimental data from the magnetic measurements of the short model magnets along with the feed- back from coil fabrication [17,18].

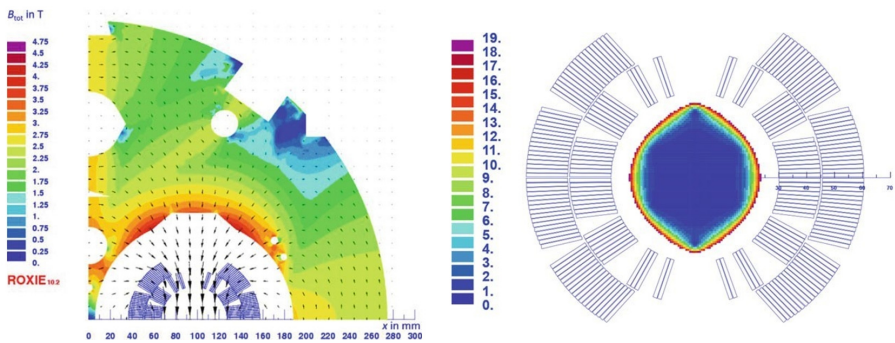

(a) (b)

Fig. 4. (a) Two-in-one model used for coil optimization; (b) coil cross-section, with relative field errors in units.

The nature of the magnetic flux pattern in the two-in-one yoke configuration requires additional features to minimize the cross-talk between the apertures, in particular for the b_2 component. The two holes in the yoke insert reduce the b_2 variation from 16 units to 13 units. Such large cross-talk indicates that the distance between the apertures and the overall size of the yoke would ideally need to be increased for such a high field magnet.

Due to the stronger iron saturation effect, the Nb_3Sn 11 T dipole magnets will be stronger than the LHC MB at intermediate excitation levels, the peak difference being 2.4 T.m at 6.7 kA. This difference can be compensated with the foreseen 250 A bi-polar trim power converters to be installed across the 11 T dipole magnets.

Owing to the larger filament size in Nb_3Sn strands when compared to Nb—Ti strands, the scaled b_3 component due to the persistent currents in the 11 T dipole magnet is about 44 units at the LHC injection current [14]. The magnetization effects strongly depend on the current pre-cycle and the lowest current reached during the cycle, the so-called reset current, I_{res}. Using I_{res} of 100 A – being the standby current of the main dipole converters - the sextupole component can be reduced to stay within 20 units between injection (I_{inj}) and nominal current (I_{nom}), which is acceptable for the LHC [5]. In addition, as shown by the measurements, flux jumps strongly affect the filament magnetization below 1 T and reduce the projected b_3 effect, which is a beneficial effect at the expense of reproducibility.

2.4. *Mechanical Design*

The mechanical structure of the magnet provides optimum clamping of the superconducting coil in order to achieve minimum distortion of the conductor and avoid cable displacement, whilst maintaining at all times the stresses at an acceptable level for the strain sensitive and brittle Nb_3Sn. A detailed structural analysis was carried out to explore the optimal parameter space for the magnet assembly [15].

The design of the magnet was inspired by the 1-m-long LHC MFISC model magnet [6]. One of the main challenges of the mechanical design is to achieve a delicate balance between the risk of overloading the mid-plane turns and that of unloading the pole turns at full field. To enable a better control of coil stress, it was decided to rely on a removable pole [2]. Such a pole enables an

adjustment of the coil pre-compression by the insertion of bespoke shims of which the thickness is determined as a function of the coil size measured after vacuum pressure impregnation. An additional Cu-alloy filler wedge, which is potted together with the coil, is added to the outer layer to match the azimuthal size of the inner layer to simplify the pole wedge geometry as shown in Figure 5. In order to smoothen out the stress distribution between the inner and the outer layers and to reduce peak stresses in the coil along its interface with the pole during collaring, 2-mm-thick stainless-steel loading plates are added at the pole prior to impregnation.

The collared coils are assembled between the yoke halves and the central yoke laminations insert, and the two 15-mm-thick stainless-steel outer shells. The shells are welded together in a welding press to form the shrinking cylinder.

3. 11 T Dipole Development at CERN

The joint 11 T dipole R&D program at CERN started in 2011 with the transfer of the technology developed at FNAL, and with adjustments to the LHC MB specific design features [7]. At CERN, development was undertaken having in mind a technology suitable for scaling up to the long magnets for installation in the accelerator. In parallel to the R&D, the large tooling for the manufacturing of the long magnets was designed, procured, and installed in the CERN Large Magnet Facility.

3.1. *CERN Model Design, Fabrication and Training*

Twenty-three 2 m long coils were fabricated during the period of 2013–2018 and assembled in eight single-aperture and two two-in-one-aperture short models as shown in Figure 7, with several variants explored, including different strand types, assembly parameters and procedures, and the type of quench protection heaters [15].

The single-aperture magnets were trained at nominal conditions at 1.9 K with a ramp rate of 10 A/s. Some of the models included coils that were already trained in a previous assembly. The training curves are shown for the assemblies made from virgin coils (see Figure 8). In the case of magnets SP101 and SP104, the large number of training quenches and the performance limitations

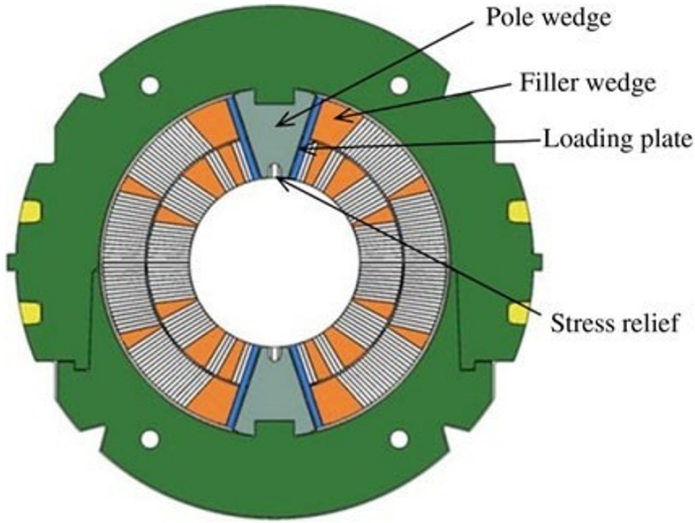

Fig. 5. Collared coil cross section.

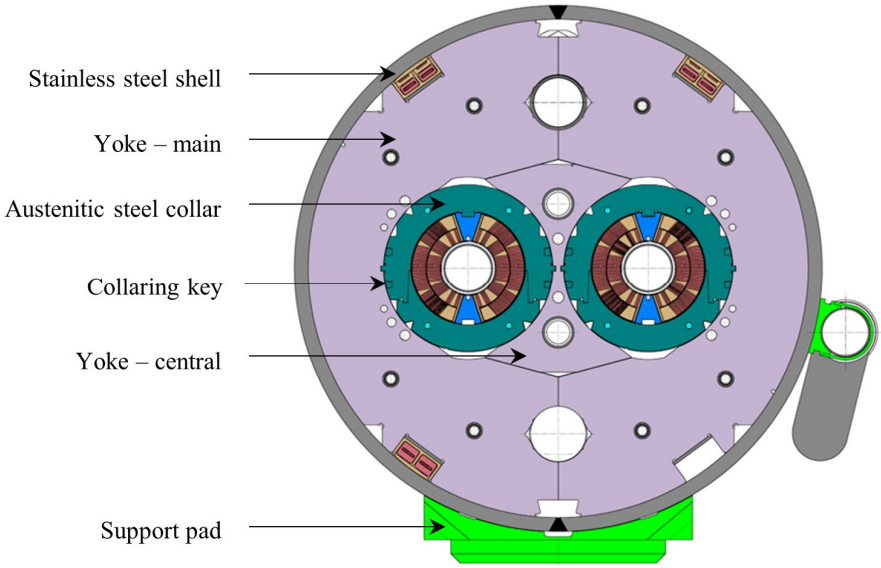

Fig. 6. Magnet cross section.

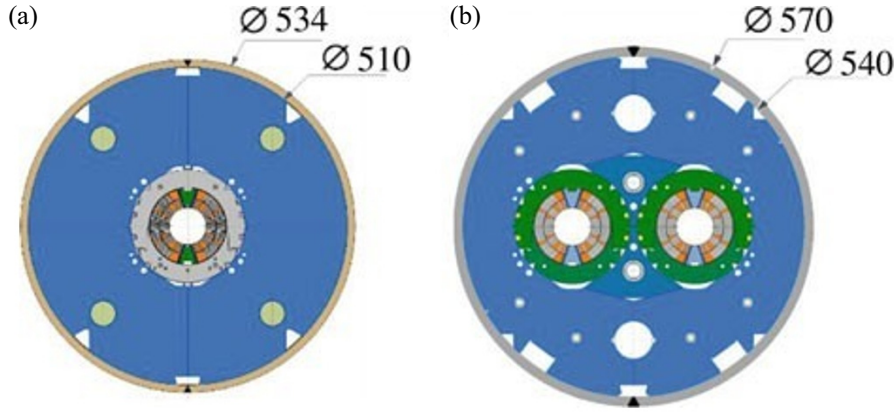

Fig. 7. CERN 11 T dipole cross-sections: (a) single-aperture; and (b) two-in-one-aperture. Dimensions are given in mm.

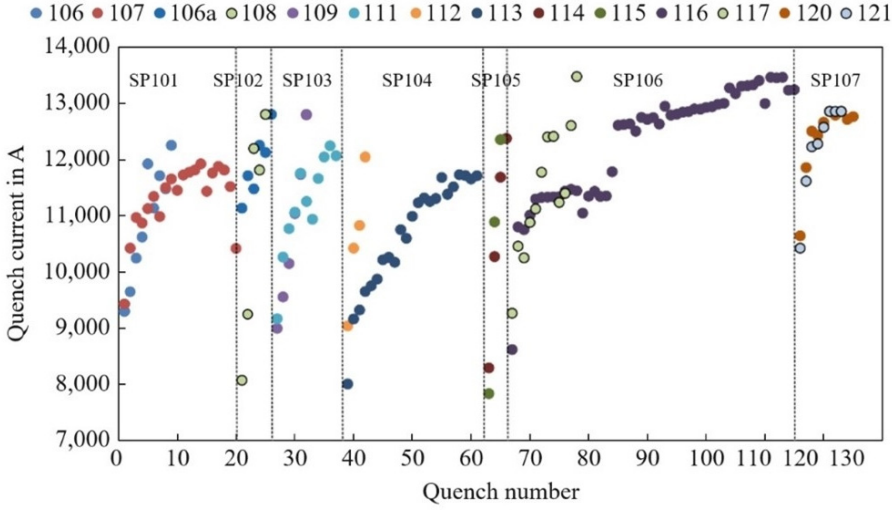

Fig. 8. Training quenches for all coils tested.

are believed to be related to issues with the layer jumps of Coils 107 (for SP101) and 112 (for SP104). There is a strong suspicion of a local non-homogeneous defect in or close to the layer jump, which may have influenced the training rate [8]. The particularly slow training of Coil 116 (SP106) may be linked with an issue in coil Block 3 of the inner layer. Following

Quench 19, as shown in Figure 8, the high MIITs (1 MIIT = 10^6 A^2.s) studies (part of the regular test program) started, and the protection was delayed, resulting in an increase of the hot-spot temperature during a quench. While additional conductor degradation driven by the hot-spot temperature was expected, the performance increased step by step, possibly due to a stress redistribution in the conductor. This magnet reached eventually 13.5 kA, with a central field of nearly 13 T.

In November 2017, a Task Force was established to review the assembly procedures of the model magnets. The Task Force focused on optimizing the collaring process parameters to cap the peak stress experienced by the coil to a value lower than 150 MPa. Model magnet SP107 was produced following the Task Force recommendations and underwent endurance testing, including 5 warm-up-cooldown (WUCD) to LHe, 10 WUCD to LN2, and over 450 electromagnetic (EM) cycles. As shown, in Figure 9 below, the magnet repeatedly achieved nominal current, and went 3 times to ultimate current, thereby confirming design feasibility.

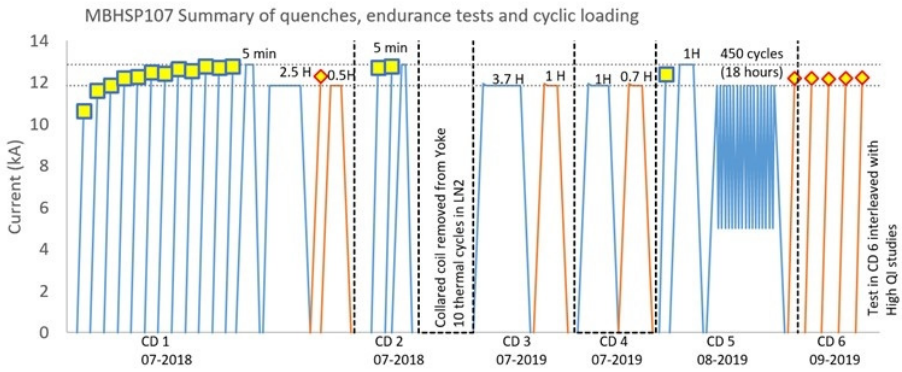

Fig. 9. Powering and quench history of model magnet SP107 issued from the 11 T Task Force (November 2017-July 2018).

3.2. *Full-Scale Prototype*

As a step towards scaling up the design and processes, a full-length prototype has been fabricated at CERN [10] (see Figure 10). This prototype had already the most relevant features of the final magnets (while still using a different type

of layout for the strands, the magnetic length not yet being optimized and, of course, not including the modifications subsequently introduced by the 11 T Task Force's revised design and procedures to address the limitations observed in the model coils). It has been a key learning and debugging exercise for such a complex object: indeed, this 5.5 m long dipole is the first long Nb_3Sn magnet built at CERN, aimed at providing a key demonstration of Nb_3Sn technology in an operating accelerator.

Fig. 10. The first 5.5 m long 11 T MBH dipole prototype in its cryostat at CERN ready to betransported to the test bench.

The prototype was targeting full accelerator quality in terms of quench performance, field errors, electrical robustness, protection, and geometry. Although most of the major tooling was available at CERN, recovered from the production of the Nb-Ti magnets for the LHC, significant modifications and upgrades were necessary. The largest additional tooling required to fabricate the coils were an argon oven for the reaction of the Nb_3Sn coils, and a vacuum pressure impregnation system. The design and procurement of the

contact tooling started in the middle of 2013 with the winding mandrel and curing mold, followed by the reaction fixture and impregnation mold, to finish later with the collaring tooling. Because of a tight schedule resulting from the initial project goal to install the magnets during the accelerator's Long Shut Down 2 (LS2) taking place during the years 2019–2020, an important overlap between the different phases of the project was inevitable. The assembly work profited from the large amount of experience in the assembling and collaring of long coils and the assembly of long cold masses at CERN for the LHC magnets. The magnet performance at 1.9 K appeared limited to about 8.5 kA in one of the coils which was likely due to a non-conformity (misplacement of coil end spacers) observed at the end of the reaction heat treatment and resulting in a relative movement between a coil block and an end spacer). Also, the prototype was assembled prior to the Task Force's assessment.

3.3. *Series production*

The series production of the 11 T magnets comprises four 2-in-1 magnets for installation in the LHC machine and two spare magnets. For this, 12 collared coils were to be produced and the initial plan foresaw the production of 30 single coils, of which six coils could be used to cover for possible incidents during production.

In order to cope with the tight schedule requirements, following competitive tendering, a service contract was placed with Alstom Power Services, Belfort, France, now part of General Electric. The work has been carried out at CERN in the Large Magnet Facility, where all of the necessary machines and tooling were available from the prototyping phase. All of the components and consumables have been provided by CERN. The other construction activities, like the cold mass assembly, the cryostating, the cold tests, and the final preparation prior to installation in the accelerator, were carried out by a mixed team of CERN personnel and contract labor under direct CERN technical responsibility.

The manufacture of the series collared-coil assemblies integrated all the lessons learned from the 11 T Task Force, in particular, the use of graded shims with 25 μm steps (see Section 2.4) to compensate the longitudinal variations of the azimuthal coil sizes measured after vacuum pressure impregnation, and a revised cable insulation scheme. The fiberglass braiding

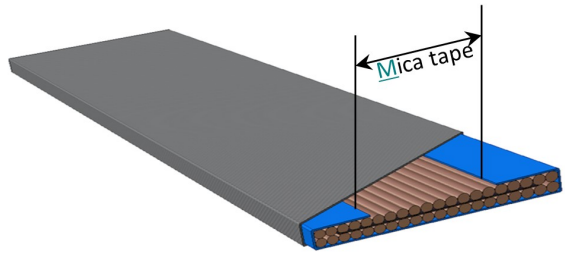

Fig. 11. Schematic view of the cable insulation. In blue, the mica tape with a gap to allow resin penetration, and in grey, the braided fiberglass.

parameters were revised in order to achieve the target thickness of 100 μm under a compression of 5 MPa (see Section 2.3). The cable insulation was actually too thick with the original braiding parameters, in the range of 135 μm at 5 MPa. Furthermore, the relatively large gap of the C-shaped mica tape, initially of 7 mm in order to facilitate resin penetration, was implying stress concentration along the edges of the cable. This gap was reduced to 1 mm with visible smoothening of peak stress (see Figure 11). It was also verified that such a reduced gap was still allowing satisfactory impregnation conditions.

Also, it should be noted that the prototype, hybrid, S1 and S2 magnets rely on quench heaters which are impregnated with the coils, while all the subsequent magnets rely on external quench heaters like in LHC dipole magnets. The decision of taking the quench heaters out of the coils was taken in early 2019 to improve quench-heater -to-coil insulation and robustness.

In addition to a hybrid assembly, which reused the structure of the prototype, but where the collared-coil assembly with the limiting coil was replaced by the first collared-coil assembly produced by Alstom Power Services/GE, a total of five series magnet assemblies have been completed (S1 through S5). The hybrid assembly and the first four cryomagnets (S1 through S4) have been tested at nominal conditions at 1.9 K in the SM18 magnet test facility. The cold mass of the fifth magnet (S5) is completed and ready for cryostating. Two more magnets (S6 and S7) are in different stages of production (from coils to collared coil). In the case of the hybrid assembly, only the new aperture was connected electrically and powered.

The new aperture of the hybrid assembly initially achieved nominal current in 2 quenches and ultimate current in 5 quenches, but exhibited detraining after a warm-up cool down cycle, with all quenches (but one) located at the

connection side of one coil head. Analysis of the WUCD procedure showed that the magnet had been subjected to large temperature gradients (in excess of 200 K), with the thermal front first hitting the magnet end where the detraining quenches originated. The procedure was subsequently changed and a maximum ΔT of 30 K was imposed on subsequent long magnets.

Three (S1, S2, S4) out of four cryomagnets reached stable nominal performance with the requested margin (11850+100 A) after the first cooldown. Initial training was relatively fast (requiring on average 2 to 4 quenches). As illustrated in the Figure 12 below, S1 passed all mandatory LHC magnet acceptance tests in July 2019 and underwent ~340 power cycles to maximum current and 1 WUCD. The performance of S3, on the contrary, appeared somewhat erratic around the nominal current, with the problematic quenches originating in the same coil (see Figure 13).

In May 2020, it was observed that S2 exhibited a limitation in quench current close to the nominal value (> 11.5 kA) following intensive reliability studies with provoked quenches and two nominal thermal cycles as part of performance validation (under nominal temperature gradient for WUCD with a $\Delta T < 30$ K). In October 2020 it was observed that S4 also exhibited a - what appears to be - permanent degradation of quench current after the first thermal cycle. These results may point to a performance degradation driven by thermo-mechanical effects triggered by the combination of powering and thermal cycles, only visible in long magnets.

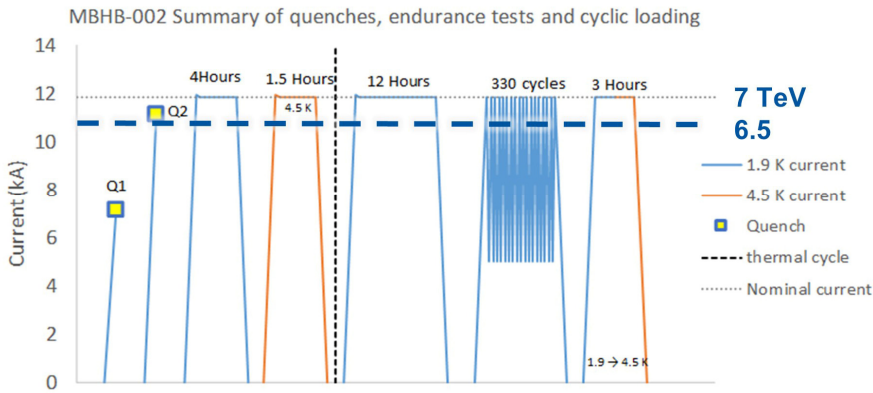

Fig. 12. Powering and quench history of first, twin-aperture, 5.5-m-long series magnet S1.

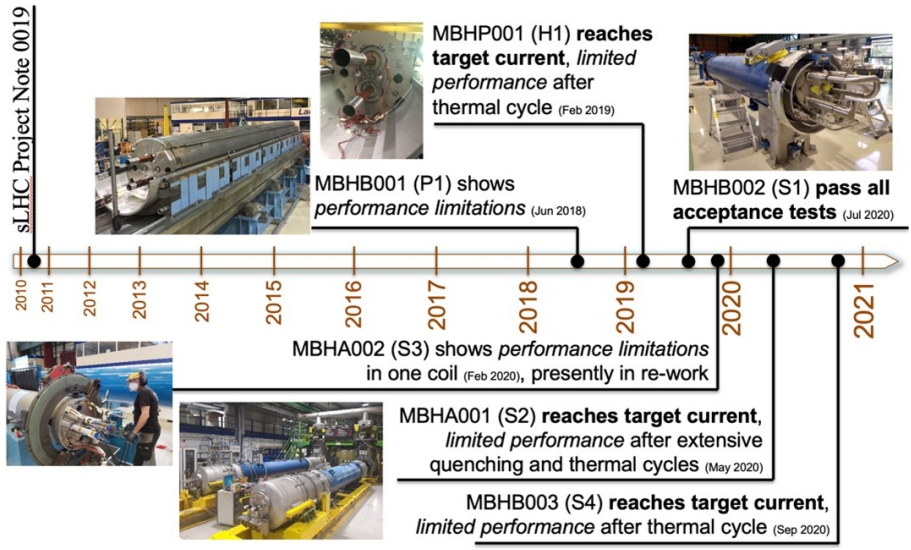

Fig. 13. Timeline of full-size 11 T dipole magnet production and cold testing.

In view of these observations, magnet testing was suspended and the installation of the 11 T dipole magnets during LS2 was given up and deferred to until after the observed degradation effect has been understood. A plan has been devised to fully understand and address the root cause of this degradation in order to assure the fully reliable operation of these magnets as well in the accelerator environment. This evaluation process has been launched at CERN at the beginning of 2021 and is still ongoing at the time of writing for this chapter.

References

1. Rossi L (2004) Experience with LHC magnets from prototyping to large scale industrial production and integration. In: Proceedings of EPAC2004. 9th European particle accelerator conference, Lucerne, July 2004, LHC Project Report 730. CERN, Geneva, p 118B. W. Bestbury, R-matrices and the magic square, J. Phys. A. 36(7), 1947–1959, (2003). ISSN 0305-4470.
2. Karppinen M, Andreev N, Apollinari G et al (2012) Design of 11 T twin-aperture Nb3Sn dipole demonstrator magnet for LHC upgrades. IEEE Trans Appl Supercond 22(3):4901504. https://doi.org/10.1109/tasc.2011.2177625.

3. Zlobin AV, Andreev N, Apollinari G et al (2012) Design and fabrication of a single-aperture 11 T Nb3Sn dipole model for LHC upgrades. IEEE Trans Appl Supercond 22(3):4001705. https://doi.org/10.1109/tasc.2011.2177619.
4. Auchmann B, Karppinen M, Kashikhin VV et al (2012) Magnetic analysis of a single-aperture 11 T Nb3Sn demonstrator dipole for LHC upgrades. In: Proceedings of IPAC2012: international particle accelerator conference, New Orleans, p 3596, (May 2012).
5. Holzer B (2014) Impact of Nb3Sn dipoles on the LHC lattice and beam optics, CERN ACC-NOTE- 2014-0063. CERN, Geneva.
6. Ahlbäck J, Ikäheimo J, Järvi J et al (1994) Electromagnetic and mechanical design of a 56 mm aperture model dipole for the LHC. IEEE Trans Magn 30(4):1746–1749. https://doi.org/10.1109/20.305594.
7. Savary F, Apollinari G, Auchmann B et al (2015) Design, assembly, and test of the CERN 2-m long 11 T dipole in single coil configuration. IEEE Trans Appl Supercond 25(3):1–5. https://doi.org/10.1109/tasc.2015.2395381.
8. Willering GP, Bajko M, Bajas H et al (2017) Cold powering performance of the first 2 m Nb3Sn DS11T twin-aperture model magnet at CERN. IEEE Trans Appl Supercond 27(4):1–5. https://doi.org/10.1109/tasc.2016.2633421.
9. Willering G, Bajko M, Bajas H et al (2018) Comparison of cold powering performance of 2-m-long Nb3Sn 11 T model magnets. IEEE Trans Appl Supercond 28(3):1–5. https://doi.org/10.1109/tasc.2018.2804356.
10. Savary F, Bordini B, Fiscarelli L et al (2018) Design and construction of the full-length prototype of the 11-T dipole magnet for the high luminosity LHC project at CERN. IEEE Trans Appl Supercond 28(3):1–6. https://doi.org/10.1109/tasc.2018.2800713.
11. D. Schoerling, A. V. Zlobin (eds.), *Nb3Sn Accelerator Magnets,* Particle Acceleration and Detection, https://doi.org/10.1007/978-3-030-16118-7_9.
12. O. Brüning et al, *LHC Full Energy Exploitation Study: Upgrade for Operation Beyond Ultimate Energy of 7.5TeV*, CERN-ACC-2020-0015.
13. G. de Rijk, A. Milanese, E. Todesco, "*11 Tesla Nb3Sn dipoles for phase II collimation in the Large Hadron Collider*", sLHC Project Note 0019, 2010.
14. S. Izquierdo Bermudez, L. Bottura, and E. Todesco, "*Persistent-Current Magnetization Effects in High-Field Superconducting Accelerator Magnets*", IEEE Transactions on applied superconductivity, Vol. 26, No. 4, (June 2016).
15. P. Ferracin, L. Bottura, A. Devred et al, "Mechanical analysis of the collaring process of the 11T dipole magnet", IEEE Transactions on applied superconductivity, Vol. 29, No. 5, (August 2019).
16. S. Izquierdo Bermudez et al, "*Mechanical analysis of the Nb3Sn 11 T dipole short models for the High Luminosity Large Hadron Collider*", 2019 Supercond. Sci. Technol. 32.
17. L. Fiscarelli, B. Auchmann, S. Izquierdo Bermudez, B. Bordini, O. Dunkel, M. Karppinen, C. Loffler, S. Russenschuck, F. Savary, D. Smekens, and G. Willering, "*Magnetic Measurements and Analysis of the First 11-T Nb3Sn Dipole Models Developed*

at CERN for HL-LHC", IEEE Transactions on applied superconductivity, Vol. 26, No. 4, (June 2016).

18. Lucio Fiscarelli, Susana Izquierdo Bermudez, Olaf Dunkel, Stephan Russenschuck, Frederic Savary, and Gerard Willering, "*Magnetic Measurements and Analysis of the First 11-T Nb3Sn 2-in-1 Model for HL-LHC*", IEEE Transactions on applied superconductivity, Vol. 27, No. 4, (June 2017).